



Identification of wind turbine main shaft torsional loads from SCADA measurements using an inverse problem approach

W. Dheelibun Remigius¹ and Anand Natarajan¹

¹Department of Wind Energy, Technical University of Denmark, Frederiksborgevej 399, 4000 Roskilde, Denmark.

Correspondence: W. Dheelibun Remigius (drwp@dtu.dk)

Abstract. To assess the structural health and remaining useful life of a wind turbine within wind farms one would require site-specific dynamic quantities such as structural response and modal parameters. In this regard, a novel inverse problem-based methodology is proposed here to identify the dynamic quantities of the drive train main shaft, *i.e.*, torsional displacement and coupled stiffness. As a model-based approach, an inverse problem of a mathematical model concerning the coupled shaft torsional dynamics with SCADA measurements as input is solved. It involves Tikhonov regularisation to smoothen the measurement noise and irregularities on the shaft torsional displacement obtained from measured rotor and generator speed. Subsequently, the regularised torsional displacement along with necessary SCADA measurements is used as an input for the mathematical model and a model-based system identification method called the collage method is employed to estimate the coupled torsional stiffness. It is also demonstrated that the estimated shaft torsional displacement and coupled stiffness can be used to identify the site-specific main shaft torsional loads. It is shown that the torsional loads estimated by the proposed methodology is in good agreement with the aeroelastic simulations of the Vestas V52 wind turbine. Upon successful verification, the proposed methodology is applied to the V52 turbine SCADA measurements to identify the site-specific main shaft torsional loads and damage equivalent load. Since the proposed methodology does not require a design basis or additional measurement sensors, it can be directly applied to wind turbines within a wind farm irrespective of their age.

1 Introduction

Monitoring of wind turbines within wind farms is increasingly becoming very important due to the need to detect specific turbines that show anomalous behavior, plan inspections or preventive maintenance, and to compute the remaining useful life of specific structures. However, addition of new instrumentation to existing turbines, such as installation of strain gauges, accelerometers can be costly and also require repetitive calibration and synchronization of their measurement signals with the turbine computer. Most wind farm operators also do not possess the aeroelastic design parameters of their wind turbines and hence cannot simulate the mechanical loads acting on their wind turbine. Monitoring of turbine primary structures through existing Supervisory Control and Data Acquisition (SCADA) system based measurements can allow cost effectiveness and provide valuable information to the wind farm operator. Usually such monitoring through SCADA only provides information on power performance and not regarding turbine structural integrity. Here we develop mathematical models for the main shaft of a wind turbine that can determine both the coupled torsional stiffness of the main shaft and its torsional displacement in



continuous time-domain, using existing time series measurements of the rotor speed and generator speed. This is a novel methodology that can potentially benefit wind farm owners, since both the property of the structure in terms of its stiffness, and the structural response can be determined without requiring additional sensors or information from the wind turbine manufacturer.

30 There are many studies available in the literature on system identification of wind turbines (Koukoura et al., 2015; Pahn et al., 2017; Norén-Cosgriff and Kaynia, 2021). All of the studies employed output-based operational modal analysis (OMA) (Wang et al., 2016) technique on the measured structural response to estimate the modal parameters of the structure. OMA methods can be broadly classified into two categories: (i) Time domain-based methods, and (ii) Frequency domain-based methods (Zhang et al., 2010). Time-domain based OMA methods are based on the calculation of auto and cross-correlation functions
35 of the response time histories. Since they possess similar properties as frequency response functions, modal parameters can be extracted from those correlation functions. Several algorithms are available to perform this task and few such methods are natural excitation technique (NExT) (James et al., 1995), random decrement technique (RDT) (Ibrahim, 1977), auto-regression moving average vector model (ARMAV) (Andersen, 1997) and stochastic subspace identification (SSI) method (Van Overschee and De Moor, 1993). Frequency-domain based OMA methods are peak picking method, enhanced frequency domain decom-
40 position method(FDD) (Brincker et al., 2001) and frequency and spatial domain decomposition method (FSDD) (Wang et al., 2005). A recent comprehensive review on various time domain and frequency domain-based OMA methods can be found in Zahid et al. (2020). However, to the best of the authors' knowledge, there is no such study available on estimating the structural response of a wind turbine component from SCADA measurements. Thus, a novel model-based approach is proposed here for the wind turbine drive train main shaft to estimate both the structural response and the modal parameters simultaneously.

45 A mathematical model concerning the shaft torsional dynamics will be utilized to obtain the system response from SCADA measurements. In this context, the concerned mathematical model comprised of differential equations will be solved for the shaft torsional velocity. Subsequently, the main shaft torsional displacement is obtained by numerically integrating the shaft torsional velocity. However, these time integration schemes are based on time-marching algorithms, the lack of initial conditions make the displacement reconstruction an ill-posed problem (Hong et al., 2008). Further, these time marching algorithms are
50 sensitive to measurement noise and they even get amplified during the time marching procedure which results in inadmissible errors in the reconstructed displacement. Also, this inaccurate displacement leads to drastic errors in the system modal parameter estimation. Hence, one needs to go for regularisation techniques to smoothen the reconstructed displacement. Hansen (2005) discussed the nature of various ill-posed problems and presented a number of solution methodologies. Though there are many regularisation techniques available, Tikhonov, Truncated singular value decomposition (SVD), and nuclear norm are a
55 few of the popular techniques (Aarden, 2017). Among all these regularisation techniques, Tikhonov regularisation (Tikhonov, 1963) has been widely used in many engineering applications (Ronasi et al., 2011; Hào and Quyen, 2012; Bangji et al., 2017; Nieminen et al., 2011) and also it has been studied extensively in the field of inverse problems (Hansen, 2005). Hence, the same has been employed in the present work. Tikhonov regularization minimizes the error using the least-square criterion and by means of a numerical damping, it also minimizes the effect of the measurement noise.



60 Together with regularised shaft torsional displacement, the same mathematical model is utilized to obtain the shaft stiffness. For this purpose, a model-based system identification technique called the collage method is used in the present study (Kunze and Vrscay, 1999; Groetsch, 1993). The model-based collage method have been successfully applied for system identification in various differential equations based problems such as boundary value problems (Kunze et al., 2009), reaction-diffusion problems (Deng et al., 2008) and elliptic problems (Kunze and La Torre, 2016). The collage method is used to convert the
65 inverse problem of system identification into a minimization problem of a function of several variables (for example unknown system parameters) and then the corresponding minimization problem is solved using a suitable algorithm. The minimization procedure is referred to as Collage coding and it is a greedy algorithm that seeks to construct an approximate solution to a target solution in one go. Hence, unlike other inverse problem methods, one need not solve the forward problem in an iterative manner (Deng and Liao, 2009).

70 One of the key benefits of estimating the shaft torsional stiffness and displacement is that it can be used to identify the site-specific shaft torsional load and the remaining useful life (RUL) (Ziegler et al., 2018) of the main shaft. Also, the main shaft torsional load can significantly affect the fatigue performance of other drive train components such as gearbox and planetary bearings (Dong et al., 2012; Gallego-Calderon and Natarajan, 2015; Ding et al., 2018). Hence the same site-specific torsional load can also be used to quantify the RUL of gearbox and other drive train components as well. Also, several older turbines
75 possess only SCADA measurements by default and they lack measurement sensors, the proposed methodology can be used for estimation of the site-specific loads of them.

The rest of the paper is organised as follows: the problem formulation consisting of the Tikhonov regularisation and the collage method is given in section 2; section 3 presents the verification of the proposed formulation; application of the proposed formulation on measurements are presented in section 4.

80 2 Problem formulation

As mentioned in the previous section, the main objective is to identify the shaft torsional displacement and coupled stiffness from SCADA measurements. This is achieved by solving the shaft torsional dynamical equations using a suitable inverse problem algorithm and the estimated shaft torsional displacement θ and torsional stiffness K will be utilized for the shaft torsional load estimation. For this purpose, a two-mass model (refer Fig. 1) (Boukhezzar et al., 2007; Berglind et al., 2015)
85 which governs the main shaft torsional dynamics subjected to the rotor and generator torques T_r and T_g , respectively, is considered, and the mathematical model is given by Eqs. (1-3). It is assumed that the gearbox is perfectly stiff while transferring deformations on the main shaft and the gear ratio, N is only considered as a parameter to proportionally adjust the force and torsional displacement between the high-speed and main shafts. The main shaft is modelled by an inertia free viscously damped torsional spring. Further, the edgewise flexibility of the blade and the torsional stiffness of the main shaft is assumed to be

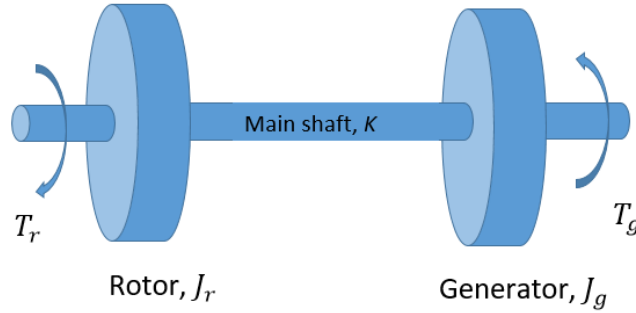


Figure 1. A two mass model of wind turbine drive train.

90 combined in K .

$$J_r \dot{\omega}_r = T_r - K\theta - C\dot{\theta}, \quad (1)$$

$$J_g \dot{\omega}_g = -T_g + K/N\theta + C/N\dot{\theta}, \quad (2)$$

$$\dot{\theta} = \omega_r - \omega_g/N. \quad (3)$$

95 Here, J_r represents the inertia of the rotor, J_g represents the collective inertias of the high-speed shaft, the gearbox, and the generator, ω_r and ω_g are the rotor and generator speeds, respectively, C is the shaft damping coefficient and θ is the shaft torsional displacement.

For normal operation of the wind turbines, the shaft torsional dynamics is mainly influenced by the low frequency modes such as blade edgewise and shaft free-free modes and the high frequency gearbox dynamics do not play a significant role in it. Hence, the two-mass model is sufficient enough to model the shaft torsional dynamics for the wind turbine normal operations as it includes both the low frequency modes. Also, given the system parameters and rotor and generator torques, the two-mass model is capable of predicting the shaft torsional displacement (θ) as close as that of the full-fledged aeroelastic simulation as shown in Fig. 2. Here, the aeroelastic simulation is performed in the DTU in-house tool called HAWC2 (Larsen and Hansen, 2007) and the results are obtained for the Vestas V52 (Vestas) wind turbine at a mean wind speed of 8 m/s.

105 In forward problem approach, given the modal parameters (J_r, J_g, C, K) and external torques (T_r and T_g), Eqs (1-3) are solved for ω_r, ω_g and θ . But given only SCADA measurements, one has to solve Eqs. (1-3) inversely for θ and modal parameters. In general, the available SCADA measurements are $\omega_r, \omega_g, P, \beta, U$. Here, P, β, U are, respectively, the generator power, blade pitch angle and wind velocity.

2.1 Collage method

110 Given ω_r and ω_g , it is straightforward to use Eq. (3) to obtain $\dot{\theta}$ and then θ . The next step is to estimate the modal parameters that are required for the load calculation. The collage method (Kunze and Vrscay, 1999; Groetsch, 1993) is used for the same

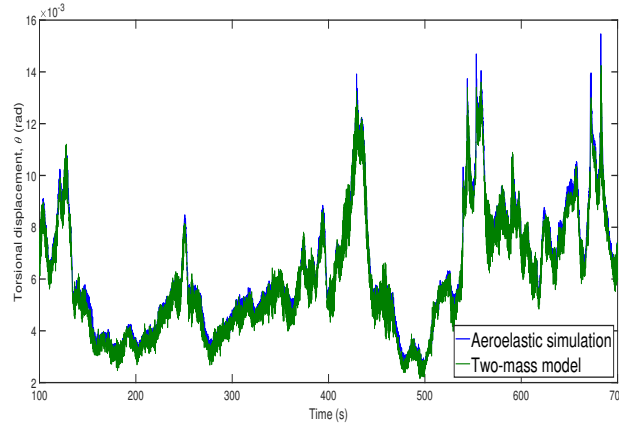


Figure 2. Comparison of the estimated shaft torsional displacement (θ) with the aeroelastic simulation result.

in the present study since it is a model-based approach. For a given initial value problem (IVP),

$$x(t) = f(x, t), x(0) = x_0, \quad (4)$$

that admits a target solution $x(t)$, the associated Picard integral operator T is given by,

$$(Tu)(t) = x_0 + \int_0^t f(u(s), s) ds. \quad (5)$$

115 The assumptions regarding the parameter estimation problem using the collage method are listed as follow (Deng and Liao, 2009):

1. $x(t) \in [t_0, t_n]$ is a bounded solution; where, t_0 and t_n are positive constants satisfying $t_0 < t_n$.
2. $f_i(u, D, x, t, \lambda_1, \dots, \lambda_m)$ ($0 \leq i \leq n$) are continuous, where, λ_m is the unknown modal parameter.
3. The exact solution $x(t)$ of the system (4) exists uniquely.

120 It is important to note that the fixed point $\bar{u}(t)$ of this Picard operator is the unique solution of the given IVP (Kunze et al., 2004). Accordingly, the collage distance becomes, $(x - Tx)$ and then the optimal solution is the one which minimizes the squared collage distance *i.e.*, L^2 collage distance. Also, unlike the conventional inverse problem which minimises the approximate error $d(x - \bar{x})$, the collage method minimizes the collage distance $d(x, Tx)$ which is an useful change as one cannot find \bar{x} for a general T (Kunze et al., 2004). Further, the optimality of the collage distance minimization is ensured as
 125 shown by Kunze et al. (2004). Minimising the L^2 collage distance using least square method yields a stationarity condition, $\frac{d(x-Tx)}{d\lambda_m} = 0$, which results in a set of linear equations in terms of the unknown modal parameters (λ_m). By solving these equations, the modal parameters are estimated.

When concerning the shaft dynamics, the rotor equation (Eq. 1) cannot be used for the parameter estimation as there is no information about the rotor torque. Instead, the collage method is applied on generator equation (Eq. 2) to estimate the modal



Wind turbine	Design K (N.m)	Estimated K (N.m)	% error
DTU-10 MW	2.317E09	2.1785E09	5.98
Vestas V52	-	-	6.98

Table 1. Comparison of estimated K with design K for a turbine variant where only the main shaft is flexible.

130 parameters as the generator torque (T_g) can be readily obtained from SCADA data as, $T_g = P/\omega_g$. Accordingly, the Picard integral for Eq. (2) becomes,

$$(Tu)(t) = J_g[\omega_g - \omega_{g0}] + \int_0^t T_g dt - K \int_0^t \theta dt - C \int_0^t \dot{\theta} dt, \quad (6)$$

where, t is the time variable and ω_{g0} is the generator speed at time, $t = 0$. Modal parameters will be obtained by minimizing Eq. (6) using the least square method.

135 2.1.1 Application of the Collage method

To the best of the authors' knowledge, this collage method has not been used in the context of wind turbine system identification and hence it is important to check the applicability of this method for the same. This is done by estimating the modal parameters using the collage method for the following two wind turbines and verifying with its design values, (i) DTU 10-MW (Bak et al.) and (ii) Vestas-V52. For facilitating a comparison of the main shaft response alone, the rigid variant of the turbine is chosen
 140 and this implies that the rotor and tower are rigid and the main shaft alone is considered to be flexible. By performing HAWC2 aeroelastic simulations on these turbines, the shaft torsional displacement θ is obtained. Then, by minimising Eq. (6) concerning the modal parameters, K , C , and J_g are obtained. Since for the estimation of shaft torsional load, only K is needed among all the modal parameters, hence the same is compared with the design values. The estimated shaft stiffness and the stiffness from the aeroelastic model of the DTU 10-MW turbine along with percentage error are tabulated in Table. 1. Due to confidentiality
 145 policy, only the percentage error is given for the Vestas V52 turbine. As seen in the table, the estimated values match well with the design values. If the torsional displacement (θ) is known, then the determination of torsional stiffness (K) from Eq. (6) is readily feasible as explained. However in practice, the shaft torsional displacement is unknown, and therefore the collage equations may not be directly used to determine the shaft stiffness.

2.2 Regularisation

150 As explained earlier, with ω_r and ω_g , $\dot{\theta}$ is obtained by using Eq. (3) and then by using time integration schemes on $\dot{\theta}$, the shaft torsional displacement (θ) is obtained. However, these time integration schemes are based on time-marching algorithms, they require initial condition on displacement which are usually unavailable or inaccurate in real situations. The effect of the lack of initial conditions on the reconstructed displacement obtained using the time integration scheme is shown in Fig. 3. As seen in the figure, the numerical error is multiplicatively increased with time which results in a drift in the reconstructed
 155 displacement. As mentioned in the introduction, to minimize the numerical error due to the lack of initial conditions and to



subsidize the effect of measurement noise, a widely used regularization technique called Tikhonov regularization (Tikhonov, 1963) is employed here.

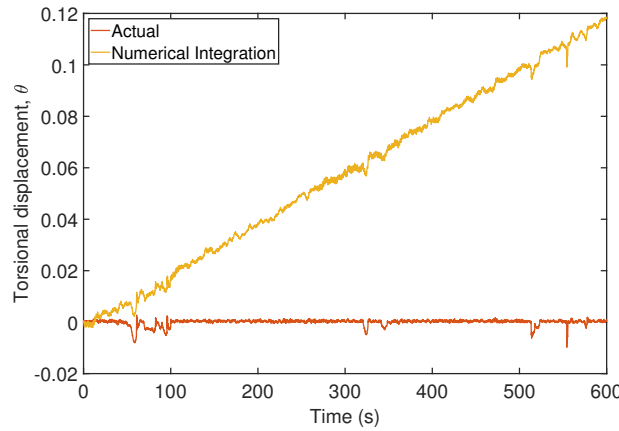


Figure 3. Comparison of time integration displacement with actual displacement.

Implementation of Tikhonov regularization on the velocity to obtain the displacement is not readily available in the literature, the same is presented here for the sake of completeness. By definition, the velocity $\dot{\theta}$ is expressed as,

$$160 \quad \dot{\theta}(t) = \frac{d\theta}{dt} \approx \dot{\hat{\theta}}(t), \quad (7)$$

where, $\dot{\hat{\theta}}(t)$ is the velocity obtained from Eq. (3) which can be considered as a measured velocity. As explained earlier, the lack of initial conditions in addition to the measurement noise leads to erroneous displacement. In order to minimise the error, following minimisation problem has to be solved,

$$\text{Min } \Pi_E(\theta) = \frac{1}{2} \int_{t_1}^{t_2} (\dot{\theta}(t) - \dot{\hat{\theta}}(t))^2 dt. \quad (8)$$

165 Here, $\dot{\hat{\theta}}$ is the calculated velocity. By means of the trapezoidal rule, Eq. (8) is discretised as follows (Hong et al., 2008),

$$\Pi_E(\theta) \approx \|\mathbf{L}_a(\dot{\theta} - \dot{\hat{\theta}})\|_2^2 \Delta t, \quad (9)$$

where Δt is the time interval of the discretization and \mathbf{L}_a is the diagonal weighing matrix of order $(n + 1)$ as,

$$\mathbf{L}_a = \begin{bmatrix} 1/\sqrt{2} & & & & & \\ & 1 & & & & \\ & & \ddots & & & \\ & & & 1 & & \\ & & & & 1/\sqrt{2} & \end{bmatrix}. \quad (10)$$



Further, the calculated velocity $\dot{\theta}$ is discretised by the central difference rule and written in matrix form as,

$$170 \quad \frac{1}{\Delta t} \mathbf{L}_c \theta = \dot{\theta}, \quad (11)$$

where, the central difference matrix \mathbf{L}_c of size $(n+1) \times (n+3)$ and the displacement vector θ of size $(n+3)$ are given as,

$$\mathbf{L}_c = \begin{bmatrix} 1 & 0 & 1 & \dots \\ -1 & 0 & 1 & \\ & \ddots & & \\ -1 & 0 & 1 & \\ \dots & -1 & 0 & 1 \end{bmatrix}, \quad \theta = \begin{pmatrix} \theta_{-1} \\ \theta_0 \\ \vdots \\ \theta_n \\ \theta_{n+1} \end{pmatrix}. \quad (12)$$

Here, the time steps denoted by -1 and $(n+1)$ are fictitious nodes. Substitution of Eq. (11) into Eq. (9) leads to,

$$\text{Min } \Pi_E(\theta) \approx \frac{1}{2} \left\| \frac{1}{2\Delta t} \mathbf{L}_a \mathbf{L}_c \theta - \mathbf{L}_a \dot{\theta} \right\|_2^2 \Delta t = \frac{1}{2} \left\| \frac{1}{2} \mathbf{L} \theta - \mathbf{L}_a \dot{\theta} \Delta t \right\|_2^2 \frac{1}{\Delta t}, \quad (13)$$

175 where, $\mathbf{L} = \mathbf{L}_a \mathbf{L}_c$. This minimisation problem is regularised for solution boundedness with a parameter λ , and given as,

$$\text{Min } \Pi_E(\theta) \approx \frac{1}{2} \left\| \frac{1}{2} \mathbf{L} \theta - \mathbf{L}_a \dot{\theta} \Delta t \right\|_2^2 + \frac{\lambda^2}{2} \|\theta\|_2^2. \quad (14)$$

The above minimisation problem is known as the Tikhonov regularisation and λ is referred to as the regularisation parameter.

Minimising Eq. (14) as,

$$\frac{d\Pi_E}{d\theta} = \frac{1}{2} \left(\frac{\mathbf{L}^2 \theta}{2} - \mathbf{L} \mathbf{L}_a \dot{\theta} \Delta t \right) + \lambda^2 \theta = 0, \quad (15)$$

180 yields the following quadratic equation in θ ,

$$\theta = \left(\frac{\mathbf{L}^2}{4} + \lambda^2 \mathbf{I} \right)^{-1} \frac{\mathbf{L} \mathbf{L}_a \dot{\theta} \Delta t}{2}, \quad (16)$$

where, \mathbf{I} is the identity matrix of order $(n+3)$. Since ten-minute SCADA measurements with a sampling frequency of 50 Hz are considered for $\theta(t)$ estimation, n becomes 30000.

The choice of regularisation parameter (λ) plays a crucial role in getting an optimal fit for the solution. Based on the
 185 knowledge about measurement errors, Hansen (2005) proposed two classes for the estimation of λ :

- methods based on knowledge of measurement errors
- methods that do not require details about measurement errors.

In the present scenario, the information regarding the measurement error is unknown, hence class two is used for the current study. In class two, there are three widely used methods (Nieminen et al., 2011): (i) quasi optimality criterion, (ii) Generalized
 190 gross validation (GCV), and (iii) L-curve method. Compared to the GCV method, the other two methods give a better estimate

of λ (Gao et al., 2016). Further, for larger problems, the quasi optimality method is computationally expensive than the L-curve method. Owing to this fact, the L-curve method is used here for estimating λ . In L-curve method, the optimal λ is the one which gives the maximum curvature in the L-curve between norm of the regularized solution $\alpha(\lambda) = \|\theta_{reg}\|_2$ and norm of the residual $\beta(\lambda) = \left\| \frac{1}{2} \mathbf{L}\theta - \mathbf{L}_a \dot{\hat{\theta}} \Delta t \right\|_2$ and the curvature of the L-curve is given by (Nieminen et al., 2011),

$$195 \quad \kappa(\lambda) = \frac{\ddot{\alpha}\dot{\beta} - \dot{\beta}\ddot{\alpha}}{[\dot{\alpha}^2 + \dot{\beta}^2]^{3/2}}. \quad (17)$$

Substituting the optimal λ obtained by finding the maximum curvature of Eq. (17) and $\dot{\hat{\theta}}(t)$ obtained from Eq. (3) in Eq. (16), the regularised displacement (θ_{reg}) is obtained. The obtained regularised torsional displacement is compared with the actual displacement in Fig. 4. Also, the displacement obtained from the numerical integration technique also presented in the same figure. As seen in the figure, result using Tikhonov regularisation matches closely with the actual displacement as compared to the displacement obtained by numerical integration.

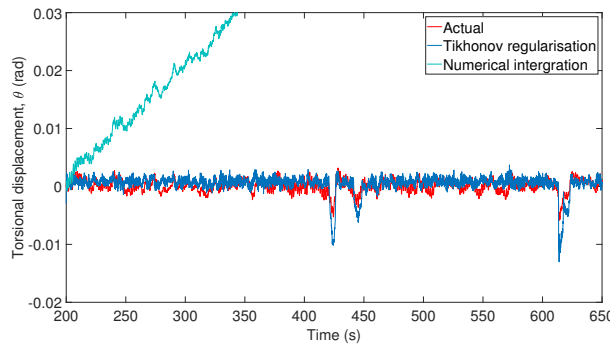


Figure 4. Comparison of the Tikhonov and time integration displacements with actual displacement.

200

Upon obtaining θ using the Tikhonov regularisation, Eq. (2) is then solved inversely with regularized θ using the collage method for the estimation of K and then the torsional load is obtained as $M_z = K\theta$. This entire methodology is shown as a flow chart in Fig. 5.

3 Verification of the method on V52 turbine simulations

205 To verify the proposed methodology for the torsional load estimation described in section 2, aeroelastic simulations are performed for Vestas V52 turbine corresponding to the design load case (DLC 1.2) (Hansen et al., 2015) in HAWC2. The DLC 1.2 consists of 18 simulations (three yaw directions and six turbulent wind seeds) for each mean wind speed and the mean wind speed is ranging from 4 m/s to 26 m/s in the interval of 2 m/s, which results in total 216 simulations. From these 216 simulations, the inputs (ω_r , ω_g , and T_g) for the proposed methods are obtained and by following the procedure depicted
 210 in Fig. 5, the torsional loads are obtained and the same is compared with the simulation results. From the simulated ω_r and

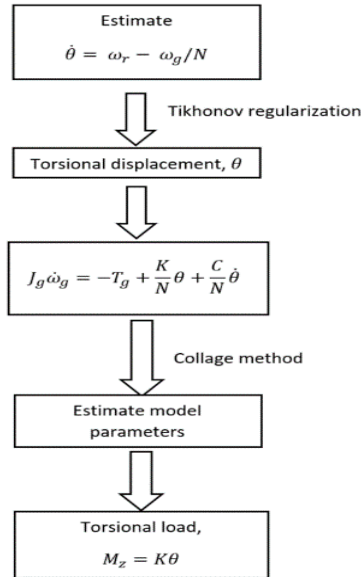


Figure 5. Flowchart depicting the inverse problem algorithm.

ω_g , the torsional velocity $\dot{\theta}$ is obtained using Eq. (3) and then the corresponding θ for each simulation is obtained by using the Tikhonov regularisation. By assuming that the same level of noise presents in all the simulations of a particular mean wind speed, the optimal λ is estimated only once per mean wind speed. The estimated regularisation parameter (λ) for each mean wind speed is presented in Fig. 6. As seen in the figure, a higher value of λ at higher wind speeds indicates that more numerical damping is needed to suppress the numerical noise.

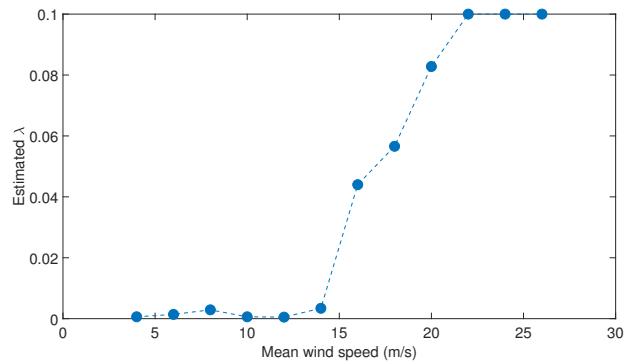


Figure 6. Estimated λ for each mean wind speeds.

215

At this point, it is important to realize that the static component of the displacement does not have any effect on the torsional velocity and hence only the dynamic component of the torsional displacement θ_{dyn} can be reconstructed from $\dot{\theta}$ using the

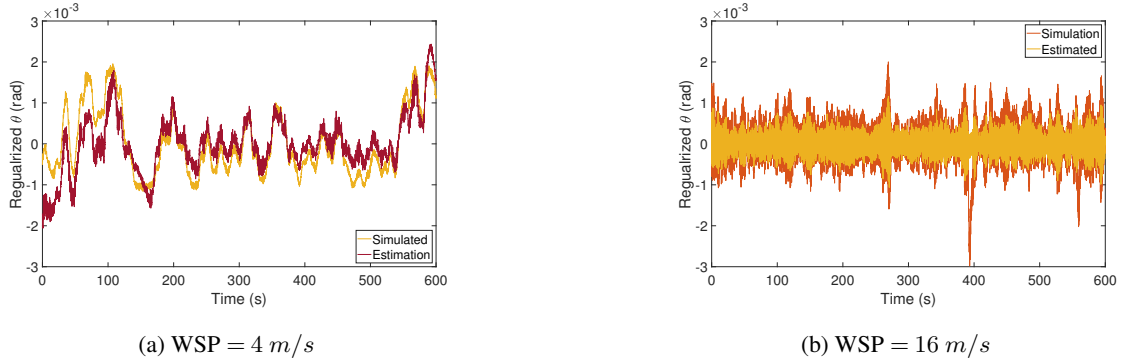


Figure 7. Comparison regularized θ_{dyn} with the results from aeroelastic simulation.

Tikhonov regularisation. The regularized θ_{dyn} for two representative mean wind speeds are compared with the dynamic component of simulated torsional displacement in Fig. 7. By removing the static displacement from the simulated displacement, the resulting dynamic component can be compared with the regularised θ_{dyn} as shown in Fig. 7. As seen in the figure, the regularised θ_{dyn} matches well with the simulated dynamic displacement for most of the time except for the peak amplitudes. After obtaining θ_{dyn} , Eq.(2) is solved inversely using the collage method for K for all the 216 simulations. Owing to uncertainty associated with θ_{dyn} estimation along with the collage method, three skewed (outliers) distributions for K can be determined at different mean wind speeds. For the distributions with outliers, mode is the better estimate of the central tendency as it is least biased by the outliers (Hedges and Shah, 2003). Ideally, there exists only one torsional K value for the wind turbine main shaft and hence by taking the mean of modes of the resulting pdfs some stability can be gained for the resultant estimate of K . The relative error between the estimated K value obtained by taking the mean of modes and the design value of the turbine is 12.06 % and the values are not presented here due to confidentiality policy. At this point, it is important to remember that the estimated K value is a combination of the main shaft and blade edgewise stiffness.

In order to obtain the site-specific torsional load, it is important to estimate the static displacement (θ_{stat}), since the torsional load is given by $M_z = K\theta = K(\theta_{stat} + \theta_{dyn})$. This is achieved by considering the static equilibrium of Eq. (1) as follows,

$$K\theta_{stat} = T_{r_{mean}} = \frac{T_{g_{mean}}}{\eta_{gen}}, \quad (18)$$

where, η_{gen} is the generator efficiency, which is 94.4 % for the V52 turbine and from Eq. (18), θ_{stat} is obtained as,

$$\theta_{stat} = \frac{T_{g_{mean}}}{K\eta_{gen}}. \quad (19)$$

Hence, by using θ_{stat} and θ_{dyn} , the total torsional load is obtained as,

$$M_z = K(\theta_{stat} + \theta_{dyn}), \quad (20)$$

At this stage, the estimated torsional loads can be compared with the simulated torsional loads. The comparison of the torsional loads for two representative mean wind speeds are shown in Fig. (8). In the figure, confidential values such as load

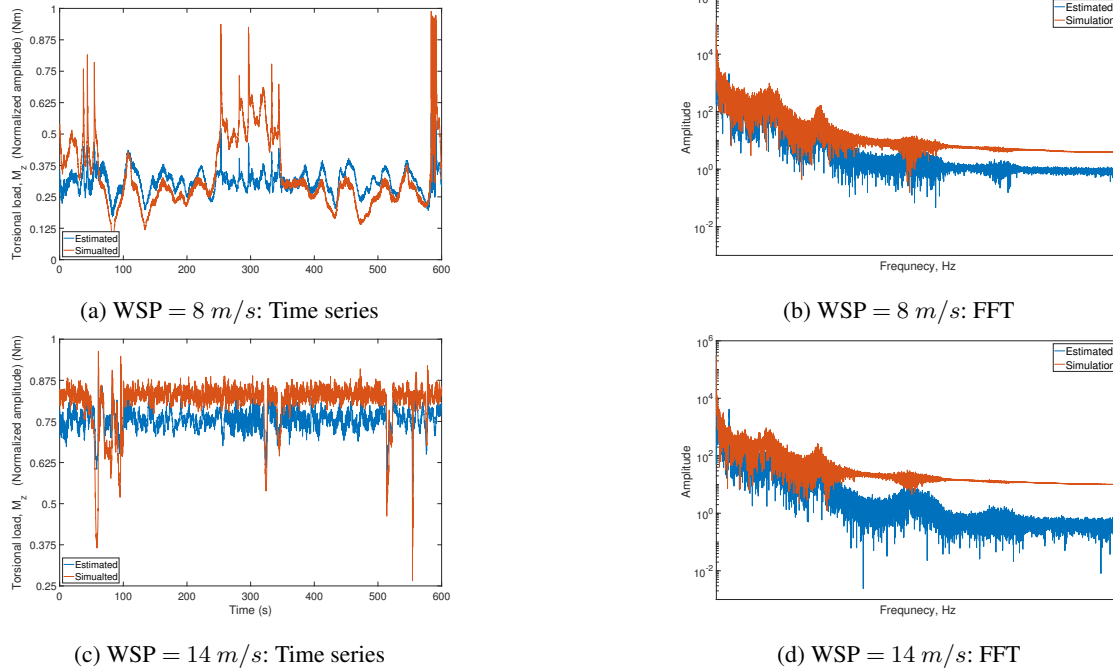


Figure 8. Comparison reconstructed time series and frequency spectra of the torsional load for two different mean wind speeds.

amplitude and frequency are not presented. As seen in the figure, all the important aspects of the time-series variation and the
 240 dominant frequency dynamics (low-frequency components - upto first three peaks) are captured quite well in the estimated
 torsional load.

Upon estimating the torsional load, the torsional damage equivalent load (DEL) at each mean wind speed is calculated using
 the following equation:

$$DEL = \left(\frac{1}{N_{ref}} \sum_{i=1}^{N_{sim}} \left(\frac{1}{N_{sim}} \right) \sum_{k=1}^{k_n} \frac{N_{i,k} S_{i,k}^m(0)}{T_{sim}} \right)^{\frac{1}{m}}, \quad (21)$$

245 where, T_{sim} is the duration of the load case, N_{sim} is the number of simulations at each mean wind speed, k_n is the total number
 of load cycles in a given time series, $N_{i,k}$ are the number of cycles at load amplitude $S_{i,k}(\sigma)$ determined with rain flow counting
 and m is the Wöhler exponent. The zero mean load amplitude is obtained as (Veldkamp, 2006), $S_{i,k}(0) = S_{i,k}(\sigma) + MS_m$,
 where, S_m is the mean load and M is the mean stress sensitivity. The turbine shaft is made up of cast iron and Veldkamp
 (2006) has reported that for such material, the mean stress correction factor is $M = 0.19$. For the 1 Hz torsional DEL of a
 250 ten-minute time series, N_{ref} becomes 600 cycles and $m = 6$ is used for the present computation. Using Eq. (21), the computed
 torsional DEL for DLC 1.2 is compared with the simulated DEL and is shown in Fig. (9). For most of the means wind speeds,
 the estimated DEL is in good agreement with the simulated DEL and the absolute error between these two at each mean wind
 speed ranges from 4% to 12 %. Higher error at higher mean wind speeds is due to the fact that the peak amplitudes in θ_{dyn} are

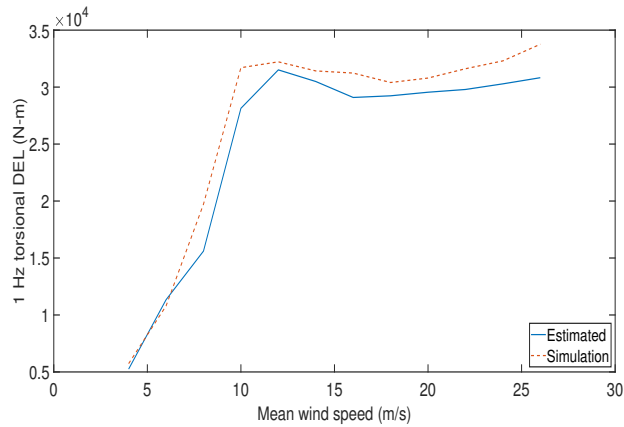


Figure 9. Comparison of the predicted DEL with the DEL computed from aeroelastic simulations over all mean wind speeds.

Minimum rotor speed	1.7 (<i>rad/s</i>)
Minimum power	100 <i>W</i>
Mean wind speed	4 (<i>m/s</i>)
Wind direction	[280°-320°]

Table 2. Normal operation filter conditions.

not captured well using the Tikhonov regularisation. This could be due to fact that the pitch control will be active beyond the
 255 rated wind speed and hence the instantaneous changes in the pitch angle affects the rotor speed.

4 Application on V52 turbine measurements

Now, using the verified methodology, the torsional loads for the drive train main shaft are estimated from the SCADA mea-
 surements. For this purpose, SCADA measurements of the Vestas V52-850 kW research turbine installed at the DTU Risø site
 will be utilized. In particular, measurements taken for the period of January 2019 consisting of 4459 ten minute recorded cases
 260 are used for this study. Since the interest is on normal operations of the turbine, the measurement data is filtered based on the
 conditions given in Table 2 that results in 627 cases.

It is important to note that based on the site sector assessment, the V52 turbine is in wake free condition between 280° and
 320° wind directions. Further, speed sensors of the rotor measures the rotational speed with a low sample rate which results in
 a piecewise constant signal. This type of signal has to be converted as a differentiable signal which is achieved by increasing
 265 the sample rate followed by a spline interpolation.

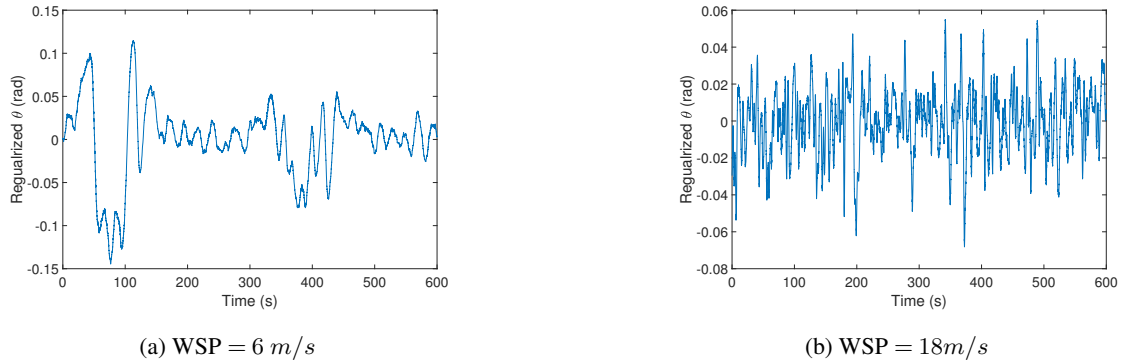


Figure 10. Regularized θ_{dyn} for two mean wind speeds.

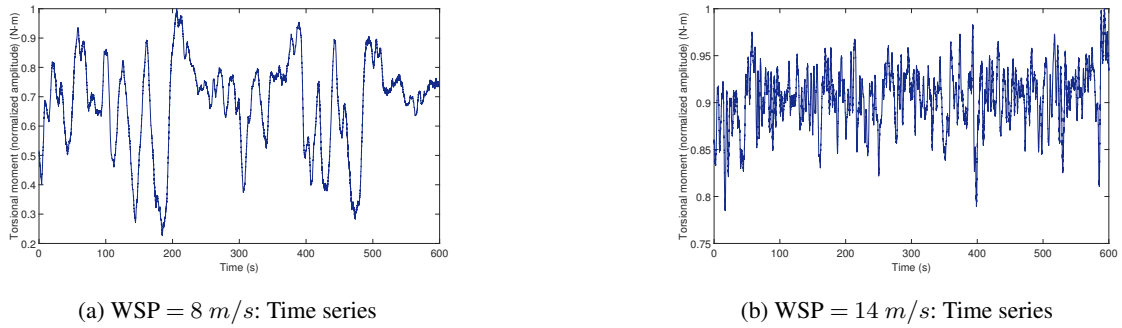


Figure 11. Identified torsional loads (M_z) for two mean wind speeds.

Now, the filtered SCADA measurements are utilized to obtain the torsional loads using the proposed methodology. Using the measured rotor speed and generator speed, θ_{dyn} is calculated using the Tikhonov regularisation method. The obtained θ_{dyn} for two representative mean wind speeds are shown in Fig. 10.

Similar to the V52 simulations, the regularisation parameter is obtained for each wind speed measurements using the L-curve criterion and the obtained values not presented here for the sake of brevity. Subsequently, by applying the collage method on Eq.(2) for all the 627 cases, the K values are estimated for each load case and then the resultant K value is obtained by taking the mean of modes of the resulting pdf as described in the previous section. The relative error between the estimated and design K values is 3.6 %. With the estimated K value, θ_{stat} is calculated for each load case using Eq. (19) and then the torsional load is obtained from Eq. (20). The calculated torsional loads for two representative wind speeds are shown in Figs. (11a, 11b). After estimating the torsional loads for all the 627 cases, the identified loads are grouped according to the mean wind speeds range from 6 m/s to 22 m/s which are subdivided into 9 wind speed bins of 2 m/s width each. Subsequently, the 1 Hz torsional DEL is calculated for each mean wind speed using Eq. (21) and the same is shown in Fig. (12). It is important to note that the DEL given in Fig. 9 (Simulation) being the design load and the DEL given in Fig. 12 being the site-specific load, the difference between these two will give an estimate about the remaining torsional fatigue life of the main shaft under normal operating conditions. Decisions regarding RUL of the drivetrain may be taken considering the estimated main shaft torsional



DEL as an input. It is also feasible to reconstruct the torsional moment time series, which may be used as an input to gearbox design tools to predict the loading within the gearbox.

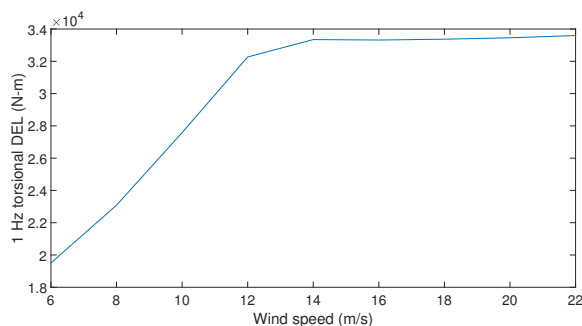


Figure 12. Estimated torsional DEL from SCADA measurements of Vestas V52 turbine.

5 Summary

A novel inverse problem-based approach is developed for estimating the shaft torsional displacement and stiffness by using the SCADA measurements. A mathematical model describing the coupled shaft torsional dynamics is used for this purpose. Numerical errors and the effect of measurement noise on the displacement reconstruction are minimized through the Tikhonov regularization technique. Subsequently, the collage method is used to estimate the main shaft coupled torsional stiffness. The estimated main shaft quantities are then used to identify the main shaft site-specific torsional load. The proposed formulation is successfully verified for the main shaft torsional loads with the aeroelastic simulation of the Vestas V52 turbine. Upon verification, the methodology is extended to identify the site-specific main shaft torsional loads of the same turbine by using SCADA measurements. For this purpose, the measurement data from the DTU Risø site is utilized and the measurement data is filtered and calibrated for the turbine normal operation. Using the identified torsional loads, the torsional DEL is obtained. Depending on the prior information about the stiffness value, one can either use the entire proposed methodology or follow the torsional displacement estimation part of the proposed methodology for the torsional load identification. Since the site-specific SCADA measurements are used in the analysis, the obtained loads can give a better estimate of the remaining fatigue life which can help in the life extension decision-making process. Besides monitoring the estimated loads can help in inspection planning and scheduling maintenance activities. As the proposed methodology does not require any design basis, it can be used for any older turbines for the estimation of the main shaft torsional RUL.

Author contributions. **W. Dheelibun Remigius:** Methodology, Formal analysis, Investigation, Validation, Writing - original draft. **Anand Natarajan:** Original idea, developing the scientific methods, Writing - review and editing, Supervision.

<https://doi.org/10.5194/wes-2021-25>
Preprint. Discussion started: 27 April 2021
© Author(s) 2021. CC BY 4.0 License.



Competing interests. The authors declare that they have no known competing financial interests or personal relationships that could have appeared to influence the work reported in this paper.

Acknowledgements. This work has been fully funded by the Energy Technology Development and Demonstration Programme, Denmark (EUDP) [Grant No. 64017 -05114]. Investigations have been carried out at Department of Wind Energy, Technical University of Denmark.



305 References

- Aarden, P.: System Identification of the 2B6 Wind Turbine: A regularised PBSIDopt approach, Master's thesis, Delft University of Technology, 2017.
- Andersen, P.: Identification of civil engineering structures using vector ARMA models, Ph.D. thesis, Department of Building Technology and Structural Engineering, Aalborg University, 1997.
- 310 Bak, C., Zahle, F., Bitsche, R., Kim, T., Yde, A., Henriksen, L. C., Natarajan, A., and Hansen, M.: Description of the DTU 10 MW reference wind turbine, Tech. Rep. I-0092, DTU Wind Energy.
- Bangji, Z., Shouyu, Z., Qingxi, X., and Nong, Z.: Load identification of virtual iteration based on Tikhonov regularization and model reduction, *Hong Kong Journal of Social Sciences*, 44, 53 – 59, 2017.
- Berglund, J. J. B., Wisniewski, R., and Soltani, M.: Fatigue load modeling and control for wind turbines based on hysteresis operators, in: 315 2015 American Control Conference (ACC), pp. 3721–3727, IEEE, 2015.
- Boukhezzar, B., Lupu, L., Siguerdidjane, H., and Hand, M.: Multivariable control strategy for variable speed, variable pitch wind turbines, *Renewable Energy*, 32, 1273–1287, 2007.
- Brincker, R., Ventura, C., and Andersen, P.: Damping estimation by frequency domain decomposition, in: Proceedings of the 19th International Modal Analysis Conference (IMAC), pp. 5–8, Orlando, FL, USA, 2001.
- 320 Deng, X. and Liao, Q.: Parameter estimation for partial differential equations by collage-based numerical approximation, *Mathematical Problems in Engineering*, 2009, 2009.
- Deng, X., Wang, B., and Long, G.: The Picard contraction mapping method for the parameter inversion of reaction-diffusion systems, *Computers & Mathematics with Applications*, 56, 2347–2355, 2008.
- Ding, F., Tian, Z., Zhao, F., and Xu, H.: An integrated approach for wind turbine gearbox fatigue life prediction considering instantaneously 325 varying load conditions, *Renewable energy*, 129, 260–270, 2018.
- Dong, W., Xing, Y., and Moan, T.: Time domain modeling and analysis of dynamic gear contact force in a wind turbine gearbox with respect to fatigue assessment, *Energies*, 5, 4350–4371, 2012.
- Gallego-Calderon, J. and Natarajan, A.: Assessment of wind turbine drive-train fatigue loads under torsional excitation, *Engineering Structures*, 103, 189–202, 2015.
- 330 Gao, W., Yu, K., and Wu, Y.: A new method for optimal regularization parameter determination in the inverse problem of load identification, *Shock and Vibration*, 2016, 7328 969–1–16, 2016.
- Groetsch, C. W.: Inverse problems in the mathematical sciences, vol. 52, Springer, 1993.
- Hansen, M. H., Thomsen, K., Natarajan, A., and Barlas, A.: Design load basis for onshore turbines-revision 00, Tech. rep., DTU Wind Energy, 2015.
- 335 Hansen, P. C.: Rank-deficient and discrete ill-posed problems: numerical aspects of linear inversion, SIAM, 1998.
- Hansen, P. C.: Rank-deficient and discrete ill-posed problems: Numerical aspects of linear inversion, vol. 4, SIAM, 2005.
- Hào, D. N. and Quyen, T. N. T.: Convergence rates for Tikhonov regularization of a two-coefficient identification problem in an elliptic boundary value problem, *Numerische Mathematik*, 120, 45–77, 2012.
- Hedges, S. B. and Shah, P.: Comparison of mode estimation methods and application in molecular clock analysis, *BMC Bioinformatics*, 4, 340 31–1–11, 2003.



- Hong, Y. H., Park, H. W., and Lee, H. S.: A regularization scheme for displacement reconstruction using acceleration data measured from structures, in: *Sensors and Smart Structures Technologies for Civil, Mechanical, and Aerospace Systems 2008*, vol. 6932, p. 693228, International Society for Optics and Photonics, 2008.
- Ibrahim, S. R.: Random decrement technique for modal identification of structures, *Journal of Spacecraft and Rockets*, 14, 696–700, 1977.
- 345 James, G. H., Carne, T. G., and Lauffer, J. P.: The natural excitation technique (NExT) for modal parameter extraction from operating structures, *Modal Analysis- The International Journal of Analytical and Experimental Modal Analysis*, 10, 260–277, 1995.
- Koukoura, C., Natarajan, A., and Vesth, A.: Identification of support structure damping of a full scale offshore wind turbine in normal operation, *Renewable Energy*, 81, 882–895, 2015.
- Kunze, H. and La Torre, D.: Computational Aspects of Solving Inverse Problems for Elliptic PDEs on Perforated Domains Using the Collage
350 Method, in: *Mathematical and Computational Approaches in Advancing Modern Science and Engineering*, pp. 113–120, Springer, 2016.
- Kunze, H., La Torre, D., and Vrscay, E.: A generalized collage method based upon the Lax–Milgram functional for solving boundary value inverse problems, *Nonlinear Analysis: Theory, Methods & Applications*, 71, e1337–e1343, 2009.
- Kunze, H. E. and Vrscay, E. R.: Solving inverse problems for ordinary differential equations using the Picard contraction mapping, *Inverse Problems*, 15, 745–770, 1999.
- 355 Kunze, H. E., Hicken, J. E., and Vrscay, E. R.: Inverse problems for ODEs using contraction maps and suboptimality of the ‘collage method’, *Inverse Problems*, 20, 977–991, 2004.
- Larsen, T. J. and Hansen, A. M.: How 2 HAWC2, the user’s manual, Tech. rep., Risø National Laboratory, Technical University of Denmark, 2007.
- Nieminen, T., Kangas, J., and Kettunen, L.: Use of Tikhonov regularization to improve the accuracy of position estimates in inertial naviga-
360 tion, *International Journal of Navigation and Observation*, 2011, 450 269–1–10, 2011.
- Norén-Cosgriff, K. and Kaynia, A. M.: Estimation of natural frequencies and damping using dynamic field data from an offshore wind turbine, *Marine Structures*, 76, 102915, 2021.
- Pahn, T.: Inverse load calculation for offshore wind turbines, Ph.D. thesis, Hannover: Gottfried Wilhelm Leibniz Universität Hannover, 2013.
- Pahn, T., Rolfes, R., and Jonkman, J.: Inverse load calculation procedure for offshore wind turbines and application to a 5-MW wind turbine
365 support structure, *Wind Energy*, 20, 1171–1186, 2017.
- Ronasi, H., Johansson, H., and Larsson, F.: A numerical framework for load identification and regularization with application to rolling disc problem, *Computers & Structures*, 89, 38–47, 2011.
- Tikhonov, A. N.: Solution of incorrectly formulated problems and the regularization method, *Soviet Mathematics - Doklady*, 4, 1035–1038, 1963.
- 370 Van Overschee, P. and De Moor, B.: Subspace algorithms for the stochastic identification problem, *Automatica*, 29, 649–660, 1993.
- Veldkamp, H. F.: Chances in wind energy: A probabilistic approach to wind turbine fatigue design, Ph.D. thesis, Faculty of Mechanical Maritime and Materials Engineering, TU Delft, 2006.
- Vestas: Vestas V52, <https://en.wind-turbine-models.com/turbines/71-vestas-v52> (08-04-2020).
- Wang, T., Zhang, L., and Tamura, Y.: An operational modal analysis method in frequency and spatial domain, *Earthquake Engineering and
375 Engineering Vibration*, 4, 295–300, 2005.
- Wang, T., Celik, O., Catbas, F. N., and Zhang, L. M.: A frequency and spatial domain decomposition method for operational strain modal analysis and its application, *Engineering Structures*, 114, 104–112, 2016.



- Zahid, F. B., Ong, Z. C., and Khoo, S. Y.: A review of operational modal analysis techniques for in-service modal identification, *Journal of the Brazilian Society of Mechanical Sciences and Engineering*, 42, 1–18, 2020.
- 380 Zhang, L., Wang, T., and Tamura, Y.: A frequency–spatial domain decomposition (FSDD) method for operational modal analysis, *Mechanical systems and signal processing*, 24, 1227–1239, 2010.
- Ziegler, L., Gonzalez, E., Rubert, T., Smolka, U., and Melero, J. J.: Lifetime extension of onshore wind turbines: A review covering Germany, Spain, Denmark, and the UK, *Renewable and Sustainable Energy Reviews*, 82, 1261–1271, 2018.